

Explaining the Disparate Stereoselectivities of *N*-Oxide Catalyzed Allylations and Propargylations of Aldehydes

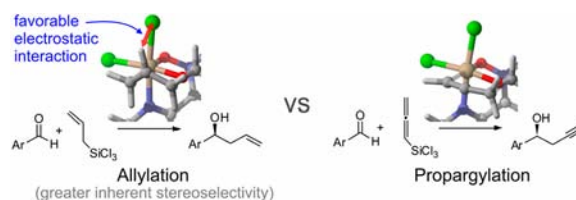
Tongxiang Lu, Mark A. Porterfield, and Steven E. Wheeler*

Department of Chemistry, Texas A&M University, College Station, Texas 77843, United States

wheeler@chem.tamu.edu

Received September 10, 2012

ABSTRACT



A simple electrostatic model explains the enhanced stereoselectivity of *N*-oxide catalyzed allylations compared to propargylations, which in turn explicates the dearth of stereoselective *N*-oxide propargylation catalysts. These results suggest that *N*-oxide catalysts that are effective for both allylations and propargylations can be designed by targeting inherently stereoselective ligand configurations and through the manipulation of distortion effects in the operative transition states.

Stereoselective allylations and propargylations of aldehydes are key C–C bond forming transformations, providing access to optically active homoallylic and homo-propargylic alcohols.¹ Of particular interest are *N*-oxide catalyzed alkylations using alkyltrichlorosilanes.² Despite the development of many effective *N*-oxide catalysts for allylations,³ there has been only one highly stereoselective *N*-oxide catalyst for the analogous propargylation reaction, published by Takenaka et al.⁴ in 2011. Moreover, *N*-oxide catalysts that are effective for allylations are generally not highly stereoselective when applied to propargylations. For example, Nakajima's bipyridine *N,N'*-dioxide^{3a} provides excellent stereoselectivities for allylations, but not for propargylations.⁵

The dearth of *N*-oxides that stereoselectively catalyze both allylations and propargylations can be contrasted with Brønsted acid catalysts for allyl- and allenylborations.⁶ For example, Antilla et al.^{6a,b} and Reddy^{6c}

showed that a single chiral phosphoric acid can stereoselectively catalyze both of these reactions. But then why have *N*-oxides, which have been so successfully exploited for allylation reactions,³ proved so much less effective in the stereoselective catalysis of propargylations?

(1) Ding, C.-H.; Hou, X.-L. *Chem. Rev.* **2011**, *111*, 1914–1937.

(2) (a) Hosomi, A.; Sakurai, H. *J. Am. Chem. Soc.* **1977**, *99*, 1673–1675. (b) Denmark, S. E.; Coe, D. M.; Pratt, N. E.; Griedel, B. D. *J. Org. Chem.* **1994**, *59*, 6161–6163. (c) Denmark, S. E.; Fu, J. P. *J. Am. Chem. Soc.* **2000**, *122*, 12021–12022. (d) Denmark, S. E.; Wynn, T. *J. Am. Chem. Soc.* **2001**, *123*, 6199–6200.

(3) (a) Nakajima, M.; Saito, M.; Shiro, M.; Hashimoto, S. *J. Am. Chem. Soc.* **1998**, *120*, 6419–6420. (b) Shimada, T.; Kina, A.; Ikeda, S.; Hayashi, T. *Org. Lett.* **2002**, *4*, 2799–2801. (c) Malkov, A. V.; Orsini, M.; Pernazza, D.; Muir, K. W.; Langer, V.; Meghani, P.; Kočovský, P. *Org. Lett.* **2002**, *4*, 1047–1049. (d) Malkov, A. V.; Bell, M.; Orsini, M.; Pernazza, D.; Massa, A.; Herrmann, P.; Meghani, P.; Kočovský, P. *J. Org. Chem.* **2003**, *68*, 9659–9668. (e) Malkov, A. V.; Bell, M.; Castelluzzo, F.; Kočovský, P. *Org. Lett.* **2005**, *7*, 3219–3222. (f) Malkov, A. V.; Ramirez-Lopez, P.; Biedermannova, L.; Rulisek, L.; Dufkova, L.; Kotora, M.; Zhu, F. J.; Kočovský, P. *J. Am. Chem. Soc.* **2008**, *130*, 5341–5348. (g) Malkov, A. V.; Barlog, M.; Jewkes, Y.; Mikusek, J.; Kočovský, P. *J. Org. Chem.* **2011**, *76*, 4800–4804. (h) Shimada, T.; Kina, A.; Hayashi, T. *J. Org. Chem.* **2003**, *68*, 6329–6337. (i) Denmark, S. E.; Yu, F. *Tetrahedron: Asymmetry* **2006**, *17*, 687–707. (j) Denmark, S. E.; Beutner, G. L. *Angew. Chem., Int. Ed.* **2008**, *47*, 1560–1638. (k) Hrdina, R.; Boyd, T.; Valterova, I.; Hodacova, J.; Kotora, M. *Synlett* **2008**, 3141–3144. (l) Kadlcikova, A.; Hrdina, R.; Valterova, I.; Kotora, M. *Adv. Synth. Catal.* **2009**, *351*, 1279–1283. (m) Vlašaná, K.; Hrdina, R.; Valterová, I.; Kotora, M. *Eur. J. Org. Chem.* **2010**, 7040–7044. (n) Kadlciková, A.; Valterová, I.; Ducháčková, L.; Roithová, J.; Kotora, M. *Chem.—Eur. J.* **2010**, *16*, 9442–9445. (o) Roithová, J.; Kadlcikova, A.; Valterova, I.; Duchackova, L.; Kotora, M. *Chem.—Eur. J.* **2010**, *16*, 9442–9445. (p) Rowlands, G. J.; Fulton, J. R.; Glover, J. E.; Kamara, L. *Chem. Commun.* **2011**, *47*, 433–435.

Here, we contrast the performance of *N*-oxides for the catalysis of allylations and propargylations based on computational studies of the model catalyst **1** as well as PINDOX, **2** (Figure 1). The data explain the disparate behavior of *N*-oxide catalysts for these reactions and also suggest strategies for the rational design of highly stereoselective *N*-oxide catalysts.

In polar solvents, the stereocontrolling TS for *N*-oxide catalyzed alkylations is a chairlike, six-membered structure featuring a hexacoordinate silicon (see Supporting Information (SI) Scheme S1).^{3a,7} These reactions are under Curtin–Hammett control, so the stereoselectivity is dominated by the relative free energies of competing TSs. Associated TS models are often constructed with the chlorines in a *trans* arrangement⁸ and the nucleophile *trans* to the *N*-oxide,^{3c,d,9} based on simple stereoelectronic arguments. However, Lu et al.¹⁰ recently showed that, for *N*-oxide catalyzed propargylations, many different ligand arrangements lead to thermodynamically accessible reaction pathways. More importantly, the relative free energies of the associated TSs are determined primarily by the ligand configurations.¹⁰ Thus, for a given catalyst, the number of possible ligand arrangements can be narrowed significantly based on their compatibility with the observed stereoselectivity. Whether these findings will also apply to allylations is examined below.

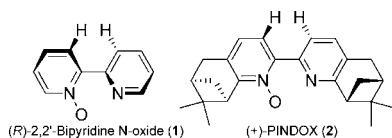


Figure 1. A model bipyridine *N*-oxide and (+)-PINDOX.^{3c}

Computations were performed at the B97-D/TZV-(2*d*,2*p*) level of theory¹¹ using Gaussian09¹² and density

(4) Takenaka, N.; Chen, J. S.; Captain, B. *Org. Lett.* **2011**, *13*, 1654–1657.

(5) Nakajima, M.; Saito, M.; Hashimoto, S. *Tetrahedron: Asymmetry* **2002**, *13*, 2449–2452.

(6) (a) Jain, P.; Antilla, J. C. *J. Am. Chem. Soc.* **2010**, *132*, 11884–11886. (b) Jain, P.; Wang, H.; Houk, K. N.; Antilla, J. C. *Angew. Chem., Int. Ed.* **2011**, *51*, 1391–1394. (c) Reddy, L. R. *Org. Lett.* **2012**, *14*, 1142–1145.

(7) (a) Hrdina, R.; Opekar, F.; Roithová, J.; Kotora, M. *Chem. Commun.* **2009**, 2314–2316. (b) Chelucci, G.; Belmonte, N.; Benaglia, M.; Pignataro, L. *Tetrahedron Lett.* **2007**, *48*, 4037–4041. (c) Sereda, O.; Tabassum, S.; Wilhelm, R. *Top. Curr. Chem.* **2010**, *291*, 349–393.

(8) (a) Musher, J. I. *Angew. Chem., Int. Ed. Engl.* **1969**, *8*, 54–68. (b) Tandura, S. N.; Voronkov, M. G.; Alekseev, N. V. *Top. Curr. Chem.* **1986**, *131*, 99–189.

(9) Traverse, J. F.; Zhao, Y.; Hoveyda, A. H.; Snapper, M. L. *Org. Lett.* **2005**, *7*, 3151–3154.

(10) Lu, T.; Zhu, R.; An, Y.; Wheeler, S. E. *J. Am. Chem. Soc.* **2012**, *134*, 3095–3102.

(11) (a) Grimme, S. *J. Comput. Chem.* **2006**, *27*, 1787–1799. (b) Becke, A. *J. Chem. Phys.* **1997**, *107*, 8554–8560. (c) Schafer, A.; Huber, C.; Ahlrichs, R. *J. Chem. Phys.* **1994**, *100*, 5829–5835. (d) Dunning, T. H., Jr. *J. Chem. Phys.* **1989**, *90*, 1007–1023.

(12) Frisch, M. J., et al. *Gaussian 09*, revision B.01; Gaussian, Inc.: Wallingford CT, 2009. See Supporting Information for full reference.

fitting. B97-D provides accurate reaction barriers while also reliably describing the noncovalent interactions present in these transition states.¹³ For example, Lu et al.¹⁰ reported excellent agreement between B97-D predictions and experimental *ee*'s for propargylations catalyzed by the helical *N*-oxide catalyst of Takenaka.⁴ Transition state structures were optimized accounting for solvent effects using the PCM model,¹⁴ and characterized by a single imaginary vibrational frequency. Reported free energies are in the solution phase. Free energies were computed at –86 °C for the model catalyst **1** (to be consistent with previous work¹⁰) and at –60 °C for PINDOX-catalyzed reactions. Lastly, energy differences among competing transition states were analyzed in terms of the distortion–interaction approach of Houk and co-workers, or, equivalently, the activation–strain model of Bickelhaupt et al.¹⁵ These analyses are based on gas-phase energies evaluated at the solution-phase geometries.

The model catalyst **1** was studied to quantify the impact of ligand configuration on the stereoselectivity of allylation reactions and to compare these results with previous work on propargylations.¹⁰ For bipyridine *N*-oxide catalyzed alkylations, there are 10 ligand arrangements that are compatible with addition of the alkyl group to the aldehyde (Figure 2). For each of these configurations, there will be a diastereomeric pair of transition states leading to either the *R* or *S* adduct. Relative TS free energies for the allylation and propargylation of benzaldehyde catalyzed by model catalyst **1** are listed in Table 1. As seen previously for propargylations,¹⁰ for allylation reactions there are many low-lying transition states, corresponding to different ligand arrangements. In other words, there is no strong preference for a *trans* chlorine arrangement, nor is it necessarily favorable for the *N*-oxide to be *trans* to the nucleophile. For a given catalyst, all TS configurations must be considered viable, and often there will be multiple accessible reaction pathways. This is in contrast to stereoelectronic arguments^{3d,4,8,9} that suggest otherwise. Moreover, for allylation reactions, all but one of these ligand configurations leads to strong selectivity for formation of either the (*R*)- or (*S*)-homoallylic alcohol, reflecting the inherent stereoselectivity of many of these ligand configurations.

Comparison of the data in Table 1 provides insight into the disparate stereoselectivities of *N*-oxide catalyzed propargylations and allylations. First, for all but one ligand configuration, **BP6**, the free energy gap between the *R* and *S* transition states is greater for allylations than for propargylations. More precisely, for *N*-oxide

(13) (a) Schenker, S.; Schneider, C.; Tsogoeva, S. B.; Clark, T. *J. Chem. Theory Comput.* **2011**, *7*, 3586–3595. (b) Goerigk, L.; Grimme, S. *Phys. Chem. Chem. Phys.* **2011**, *13*, 6670–6688.

(14) (a) Tomasi, J.; Mennucci, B.; Cammi, R. *Chem. Rev.* **2005**, *105*, 2999–3093. (b) Miertus, S.; Scrocco, E.; Tomasi, J. *Chem. Phys.* **1981**, *55*, 117–129.

(15) (a) Ess, D. H.; Houk, K. N. *J. Am. Chem. Soc.* **2007**, *129*, 10646–10647. (b) Ess, D. H.; Houk, K. N. *J. Am. Chem. Soc.* **2008**, *130*, 10187–10198. (c) Bickelhaupt, F. M.; van Zeist, W. J. *Org. Biomol. Chem.* **2010**, *8*, 3118–3127. (d) Bickelhaupt, F. M. *J. Comput. Chem.* **1999**, *20*, 114–128.

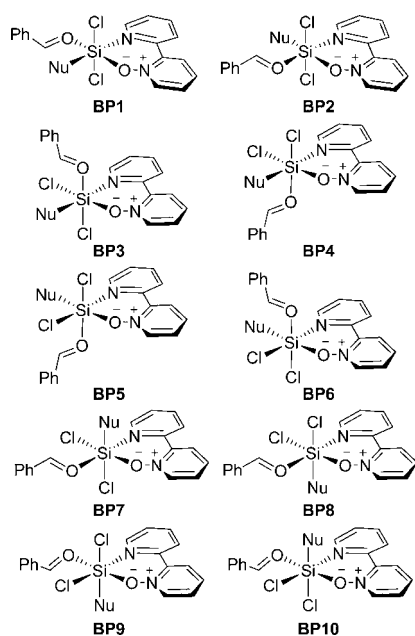


Figure 2. Ligand configurations compatible with addition of the nucleophile (Nu = allyl or allenyl) to the aldehyde for bipyridine *N*-oxide catalyzed alkylations.

catalyzed allylations there are only two ligand arrangements with free energy gaps between the *R* and *S* configurations less than 1.4 kcal mol⁻¹. This contrasts with propargylations, for which 7 of 10 ligand arrangements lead to free energy gaps smaller than 1.4 kcal mol⁻¹. This indicates that *N*-oxide catalyzed propargylations are inherently less stereoselective than allylations, which in part explains the scarcity of stereoselective *N*-oxide catalyzed propargylation catalysts. These model results also provide guidelines for the development and evaluation of TS models for *N*-oxide catalyzed alkylation reactions, as well as the design of stereoselective catalysts (*vide infra*).

One possible source of stereodifferentiation in the allylation transition states stems from electrostatic interactions within the chiral environment surrounding the silicon. In particular, the favored TS for a given ligand arrangement always features the internal vinyl C–H of the allyl group and the carbonyl C–H of benzaldehyde aligned with one of the Si–Cl bonds. This alignment should result in stabilizing electrostatic interactions (see Figure 3). In the corresponding disfavored transition states, these C–H bonds are directed away from the chlorines due to the chairlike geometry of the TS. This simple electrostatic picture also explains why propargylations are less stereoselective than allylations; the allenyl group does not have a central C–H bond, so propargylations do not benefit from the additional differentiation arising from the orientation of this bond.

To demonstrate the relevance of the above model results to real *N*-oxide catalysts, we have also studied the PINDOX catalyzed allylation^{3c} and propargylation

Table 1. Free Energy Barriers in DCM (kcal mol⁻¹), Relative to the Respective Lowest-Lying **BP1**(*R*) for the Allylation and Propargylation of Benzaldehyde Catalyzed by the Model Catalyst **1**, and the Difference between the *R* and *S* Barriers^a

	allylation			propargylation		
	<i>S</i>	<i>R</i>	diff.	<i>S</i>	<i>R</i>	diff.
BP1	0.1	0.0	0.1	0.1	0.0	0.1
BP2	4.0	2.6	1.4	2.6	3.9	-1.3
BP3	0.3	2.0	-1.7	0.7	1.9	-1.2
BP4	3.2	0.1	3.1	3.4	0.6	2.8
BP5	0.7	2.2	-1.5	0.3	0.8	-0.5
BP6	6.5	1.8	4.6	5.8	0.5	5.4
BP7	3.2	2.1	1.0	2.9	2.0	0.8
BP8	5.1	6.8	-1.7	4.2	4.3	-0.1
BP9	8.0	3.1	5.0	5.2	4.3	0.8
BP10	0.8	6.6	-5.8	0.3	5.2	-5.0

^a Propargylation data from ref 10. Note that these data are for (*R*)-2,2'-bipyridine *N*-oxide, while the data in ref 10 are for the (*S*) form.

of benzaldehyde (data for *p*-nitro- and *p*-chlorobenzaldehyde are available in the SI). *R* and *S* transition states corresponding to each of the 10 possible ligand arrangements were optimized to identify the lowest-lying transition states. Key TS structures for the allylation reaction are depicted in Figure 4; others can be found in the SI. The *S*-selectivity of (+)-PINDOX catalyzed allylations^{3c} arises from the >2 kcal mol⁻¹ free energy gap between the lowest-lying *S* transition state, (*S*)-**TS1_A**, and the lowest-lying *R*-transition states, (*R*)-**TS1_A** and (*R*)-**TS2_A**. Accounting for all possible transition states,¹⁶ we predict an *ee* of 97%, in agreement with the experimental data (*ee* = 90%).^{3c} (*S*)-**TS1_A** and (*R*)-**TS1_A** correspond to the ligand configuration in **BP5**. For the model catalyst **1**, this ligand configuration was predicted to favor formation of the *S* product by 1.5 kcal mol⁻¹ over the *R* product; this is qualitatively predictive of the 2.1 kcal mol⁻¹ gap for the PINDOX catalyzed reaction (Figure 4).

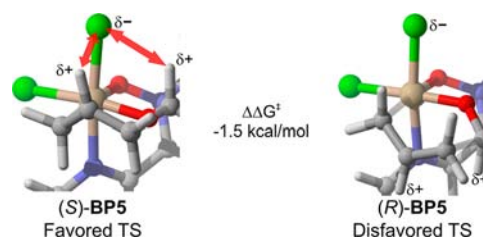


Figure 3. Exemplary TS structures for bipyridine *N*-oxide catalyzed allylation reactions, demonstrating that, for ligand arrangements with *cis* chlorines, the transition states are differentiated in part by the orientation of the allyl and carbonyl C–H bonds. Propargylations do not benefit from this effect.

(16) Ess, D. H.; Kister, J.; Chen, M.; Roush, W. R. *J. Org. Chem.* **2009**, *74*, 8626–8637.

The 2.1 kcal mol⁻¹ free energy difference between (*S*)-**TS1_A** and (*R*)-**TS1_A** is dominated by the 3.0 kcal mol⁻¹ difference in gas-phase electronic energies. This 3.0 kcal mol⁻¹ can be decomposed into a 4.9 kcal mol⁻¹ contribution from interaction energies, favoring (*S*)-**TS1_A**, offset by a 1.9 kcal mol⁻¹ difference in distortion energies, favoring (*R*)-**TS1_A** (see SI).¹⁵ The 4.9 kcal mol⁻¹ interaction energy difference arises in part from the electrostatic effects described above, in addition to the relative positions of these TSs along the reaction coordinate. In particular, in (*S*)-**TS1_A**, the length of the forming C–C bond (2.03 Å) is noticeably shorter than the corresponding bond length in (*R*)-**TS1_A** (2.08 Å). Thus, (*S*)-**TS1_A** is favored over (*R*)-**TS1_A** in part because it lies farther along the reaction coordinate.

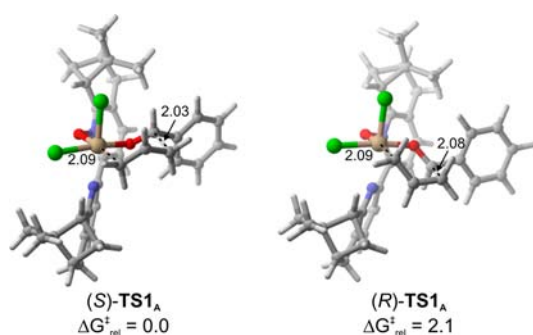


Figure 4. Low-lying TS structures and relative free energies (kcal mol⁻¹) for the PINDOX-catalyzed allylation of benzaldehyde. Bond lengths are provided in angstroms.

The TS model of Malkov et al.,^{3c} for PINDOX catalyzed allylations, which is reflective of the majority of literature on these reactions, is based on a *trans* chlorine arrangement and the allyl group being *trans* to the *N*-oxide (i.e., model system **BP2**). However, **BP2** favors the *R*-enantiomer by 1.4 kcal mol⁻¹ over the *S*-enantiomer, which is opposite of the observed selectivity for (+)-PINDOX catalyzed allylations.^{3c} In addition, computed transition states corresponding to this ligand arrangement lie considerably higher in free energy than (*S*)-**TS1_A** and are predicted not to be operative in this reaction (see SI Table S1). Moreover, consistent with the model results, these TSs predict the opposite stereoselectivity to that observed experimentally and cast doubt on the utility of the underlying stereoelectronic arguments^{3c,d,8,9} for understanding these reactions.

To explore whether PINDOX is a viable propargylation catalyst, and to further probe the applicability of the above model results, structures were also optimized for the 10 (*R,S*) pairs of TSs for the PINDOX-catalyzed propargylation of benzaldehyde. Key low-lying TSs can be found

(17) Even if the lowest lying TS corresponds to a stereoselective ligand configuration, the stereoselectivity can still be spoiled by a low-lying TS corresponding to any of the other ligand configurations.

in the SI. The two lowest-lying TSs have the same ligand configuration as found for the PINDOX-catalyzed allylation. However, in this case there is only a 0.2 kcal mol⁻¹ difference between the lowest-lying *S* and *R* TSs. Consequently, the present results predict no stereoselectivity for the PINDOX catalyzed propargylation reaction. This prediction is again in line with results from the corresponding model, **BP5**, which is predicted to be highly stereoselective for allylation reactions yet not for propargylations (Table 1). As noted above, this can be attributed in part to the lack of a central C–H bond in the allenyl group. Further analyses of this energy difference can be found in the SI.

In conclusion, *N*-oxide catalyzed allylations are inherently more stereoselective than propargylations, partly because of the presence of the internal vinyl C–H bond in the allyl group (see Figure 3). Moreover, in both of these reactions the stereoselectivity arises primarily from the arrangement of ligands surrounding the silicon. It was shown that, for propargylations, only selected ligand configurations lead to strong stereoselectivity, while for allylations nearly all of the configurations are stereoselective. Consequently, the operative reaction pathways for propargylations are less likely to pass through a stereoselective ligand configuration than for allylations, explaining why the development of *N*-oxide catalysts for asymmetric propargylations has proved so challenging. These trends were demonstrated for PINDOX, which, although highly stereoselective for allylation reactions,^{3c} is predicted to be nonstereoselective for propargylations.

The above results provide guidelines for the development of TS models for *N*-oxide catalyzed alkylations, replacing the conventional stereoelectronic arguments that pervade the literature.^{3c,d,9} They also highlight two potential strategies for the rational design of *N*-oxide catalysts. First, there are three ligand configurations predicted to provide a high degree of stereoselectivity in both allylations and propargylations, **BP4**, **BP6**, and **BP10**. A catalyst targeting any of these three configurations has the potential to be highly stereoselective for both reactions.¹⁷ Second, distortion–interaction analyses¹⁵ indicate that interaction energies tend to enhance the stereoselectivity for a given ligand configuration, particularly for allylation reactions, while distortion effects reduce the selectivity. Therefore, the manipulation of distortion energies should also serve as a strategy for the design of *N*-oxide catalysts.

Acknowledgment. This work was supported by Welch Foundation Grant A-1775, and we thank the Texas A&M Supercomputing Facility for computational resources.

Supporting Information Available. Additional figures and analysis, electronic energies, Cartesian coordinates. This material is available free of charge via the Internet at <http://pubs.acs.org>.

The authors declare no competing financial interest.